RESEARCH PAPER

Cancer Biology & Therapy 16:12, 1812–1819; December 2015; © 2015 Taylor & Francis Group, LLC

Development of a radiofrequency ablation platform in a clinically relevant murine model of hepatocellular cancer

Xiaoqiang Qi[1,2], Guangfu Li[1,2,*], Dai Liu[1,2], Anjan Motamarry[4], Xiangwei Huang[1,2], A. Marissa Wolfe[3], Kristi L. Helke[3,4], Dieter Haemmerich[5], Kevin F Staveley-O'Carroll[1,2,*], and Eric T Kimchi[1,2,*]

[1]Department of Surgery; Division of Surgical Oncology; Medical University of South Carolina; Charleston, SC USA; [2]Hollings Cancer Center; Medical University of South Carolina; Charleston, SC USA; [3]Department of Comparative Medicine; Medical University of South Carolina; Charleston, SC USA; [4]Department of Pathology and Laboratory Medicine; Medical University of South Carolina; Charleston, SC USA; [5]Department of Pediatrics; Medical University of South Carolina; Charleston, SC USA

Keywords: alanine aminotransferase (ALT), aspartate aminotransferase (AST), hepatocellular cancer (HCC), magnetic resonance imaging (MRI), murine model, radiofrequency ablation (RFA), tissue-mimicking media

Abbreviations: HCC, Hepatocellular Cancer; FDA, Food and Drug Administration; RFA, Radiofrequency ablation; Tag, SV40 T antigen; ISPL, Intrasplenic; MRI, Magnetic resonance imaging; ALT, Alanine aminotransferase; AST, Aspartate aminotransferase; H & E, Hematoxylin & Eosin; CTLA-4, Cytotoxic T-lymphocyte-associated antigen-4; PD-1, Programmed death-1

RFA is used in treatment of patients with hepatocellular cancer (HCC); however, tumor location and size often limit therapeutic efficacy. The absence of a realistic animal model and a radiofrequency ablation (RFA) suitable for small animals presents significant obstacles in developing new strategies. To establish a realistic RFA platform that allows the development of effective RFA-integrated treatment in an orthotopic murine model of HCC, a human cardiac radiofrequency generator was modified for murine use. Parameters were optimized and RFA was then performed in normal murine livers and HCCs. The effects of RFA were monitored by measuring the ablation zone and transaminases. The survival of tumor-bearing mice with and without RFA was monitored, ablated normal liver and HCCs were evaluated macroscopically and histologically. We demonstrated that tissue-mimicking media was able to optimize RFA parameters. Utilizing this information we performed RFA in normal and HCC-bearing mice. RFA was applied to hepatic parenchyma and completely destroyed small tumors and part of large tumors. Localized healing of the ablation and normalization of transaminases occurred within 7 days post RFA. RFA treatment extended the survival of small tumor-bearing mice. They survived at least 5 months longer than the controls; however, mice with larger tumors only had a slight therapeutic effect after RFA. Collectively, we performed RFA in murine HCCs and observed a significant therapeutic effect in small tumor-bearing mice. The quick recovery of tumor-bearing mice receiving RFA mimics observations in human subjects. This platform provides us a unique opportunity to study RFA in HCC treatment.

Introduction

Hepatocellular carcinoma (HCC) is the third leading cause of cancer death worldwide and continues to increase in the west, particularly the United States.[1,2] Annually it results in approximately 700,000 deaths worldwide.[3,4] Current treatments for HCC have demonstrated limited benefit as survival is poor even for patients with localized disease.[5] Surgical resection or ablation offers a small chance for cure.[6] Unfortunately, most patients are not candidates for surgical resection or even ablation due to associated liver disease.[7] Liver transplantation is an effective treatment for cirrhosis and early tumors, but as recurrence is common in advanced disease and organs are scarce, most patients are not able to receive transplantation.[8] In 2008, the receptor tyrosine kinase inhibitor, sorafenib, became the first and only drug approved by the Food and Drug Administration (FDA) to treat unresectable HCC, after it was shown to increase the median overall survival of patients from 7.9 to 10.7 months.[9] This small but statistically significant therapeutic effect highlights the challenge in treating this devastating disease. Thus, it is imperative to develop new and efficient therapeutic approaches.

Radiofrequency ablation (RFA)[10] is a minimally invasive treatment utilized in the treatment of isolated malignancies including HCC. RFA can be an effective treatment for primary liver cancer and for cancers that have spread to the liver when the patients are not suitable candidates for surgical resection. However, only small volumes of tumors can be successfully treated by RFA due to limitations with the current technology. In addition, disease progression and recurrence is often due to micrometastases that cannot be detected or eliminated by RFA. Therefore, it is

*Correspondence to: Eric T Kimchi; Email: kimchie@health.missouri.edu
Submitted: 08/07/2015; Revised: 09/02/2015; Accepted: 09/12/2015
http://dx.doi.org/10.1080/15384047.2015.1095412

extremely important to develop strategies to overcome these limitations for improving RFA efficacy in HCC treatment.

RFA may often be administered percutaneously or by laparoscopic approach. These relatively quick procedures allow for rapid patient recovery and enable the prompt resumption of other treatment strategies in patients post RFA.[11] Unfortunately, to date, strategies combining RFA with other modes of therapy have not translated into improved outcomes in patients. A major obstacle to the development of combinational strategies with RFA is the absence of clinically relevant orthotoptic animal models and an appropriate RFA generator for use in small animals.

Due to the aggressive nature of HCC and its tendency to arise in the setting of inflammation and liver fibrosis, establishing a clinically faithful model has been challenging.[12,13] We recently used an innovative approach to generate an orthotopic murine model of HCC in wild type mice.[14,15] To establish this model, histologically-normal tumorigenic hepatocytes are isolated from the MTD2 transgenic mouse line in which expression of the oncogenic SV40 T antigen (Tag) is driven by an androgen stimulated hybrid major urinary protein promoter. The androgen stimulation of the promoter occurs at the time of puberty in the mouse. These hepatocytes are transferred into the livers of prepubertal, male, syngeneic C57BL/6 mice by intrasplenic (ISPL) injection. The inoculated hepatocytes traffic and incorporate into the recipient liver through the portal vein.[14] Malignant transformation occurs gradually with stimulation of androgen and is limited to the subpopulation of transplanted MTD2 hepatocytes; this is in contrast to the MTD2 mice, which develop tumors throughout their entire liver parenchyma. Orthotopic hepatic tumors develop in 100% of the recipient mice. The developing HCC tumors can be detected and monitored for growth and treatment response with magnetic resonance imaging (MRI) 4 weeks after inoculation of MTD2 hepatocytes.

The use of radiofrequency (RF) energy to produce thermal tissue destruction has been the focus of increasing research and practice in cancer treatment for the past several years.[16] During the application of RF energy, a high frequency alternating current moves from the tip of an electrode into the tissue surrounding that electrode. This high frequency alternating current drives ions within the tissue to move and generate frictional heating. As the temperature within the tissue becomes elevated beyond 60°C, intracellular proteins are denatured and cells begin to die, resulting in a region of necrosis surrounding the electrode.[17] The decrease in tissue heating with increasing distance away from the electrode results in cylindrically shaped zones of coagulative necrosis of tissue when using monopolar simple needle electrodes. The size of the ablation is directly related to the time and temperature of the RFA.[18]

In this study, a RFA generator suitable for human therapeutic use is modified to successfully conduct liver ablation in a murine model. RFA conditions were optimized using tissue-mimicking media, and these parameters were applied to the hepatic parenchyma in wild type C57BL/6 mice. This resulted in a complete ablation of the targeted liver parenchyma in these mice. This optimized RFA technique has also been successfully translated into tumor-bearing mice, furthermore; the quick recovery of normal and tumor-bearing mice receiving RFA treatment mimics the clinical scenario that is observed in human subjects. This clinically relevant model of HCC in combination with successful application of RFA provides an ideal platform to expand our understanding of RFA's effect on HCC and explore potential RFA-integrated therapies for improving HCC treatment strategies.

Materials and Methods

Mice

Male C57BL/6 mice were purchased from the Jackson Laboratory (Bar Harbor, ME). Line MTD2 transgenic mice were kept by us that express full-length SV40 Tag driven by the major urinary protein (MUP) promoter have been previously described.[19,20] All experiments with mice were performed under a protocol approved by the Institutional Animal Care and Use Committee (IACUC) at the Medical University of South Carolina. All mice received humane care according to the criteria outlined in the "Guide for the Care and Use of Laboratory Animals."

Tissue-mimicking media for coagulation temperature measurement

A tissue-mimicking media with similar thermal and electrical properties as tissue has been developed for use with thermal therapy devices and techniques. This media was composed of 0.25% NaCl solution and 5% Agar.[21] An EPT-1000 XP™ cardiac radiofrequency generator (EPT Technologies) was used together with a 4 mm cardiac ablation catheter (7F/2.33 mm diameter),[22] with 2 additional conductors used as ground electrodes. After placing the electrodes on the gel, the gel was heated with target temperatures of 55°C – 85°C for 60 sec. During heating, surface temperature maps were obtained by an infrared imaging camera (Mikron M7500), assuming emissivity of 0.9 of the gel media.

Preparation of orthotopic murine model of HCC

An orthotopic murine model of HCC was made as described.[14] Briefly, histologically normal hepatocytes were isolated from young male Tag-transgenic MTD2 mice and seeded into the livers of male C57BL/6 mice by ISPL injection.[14]

Magnetic resonance imaging (MRI)

Tumor surveillance was conducted with MRI. All MRI scans were obtained on a 7.0 T system (Bruker Biospin, Billerica, MA, USA) with in-plan resolution 0.1 mm and slice thickness 1 mm.[14]

Radiofrequency ablation

After animals are anesthetized with inhalational isoflurane, an EPT-1000 XP™ cardiac radiofrequency generator (Boston Scientific,) equipped with a 4 mm cardiac ablation probe (7F/2.33 mm diameter) is used to perform RFA.[22] To perform RFA in murine hepatic parenchyma, two additional conductors are used as ground electrodes and placed on either side of the open abdomen. The probe is then placed on the liver surface to conduct radiofrequency ablation with defined conditions: a power output of 10 W for a duration of 60 seconds.

Preparation and hematoxylin and eosin (H & E) staining of frozen tissue section

Liver or tumor biopsies were freshly harvested from normal and tumor-bearing mice and frozen immediately by keeping tissue jar in a beaker of 2-methylbutane in dry ice. The frozen tissues were initially stored at −80°C, and transferred to −20°C on the day before sectioning on a cryostat (MICRON, HM 525, Thermo Scientific). The tissues were subjected to cryosectioning at a thickness of 10 μm and then placed on Superfrost plus slides (VWR International). Tissue sections were processed and stained with H&E as standard method. Briefly, the sections on Superfrost plus slides were stained as follows: wash in water, Richard Allan hematoxylin (VWR International) in aqueous solution for 60 s, wash in water, 1% acid alcohol for 1 dip, wash in water, 1% ammonia alcohol for 10 dips, wash in water, eosin (VWR International) for 10 s, followed by dehydration with 95%, 100% ethanol for 10 s, respectively, and xylene for 10 s.

Alanine aminotransferase (ALT) and aspartate aminotransferase (AST) measurement

Blood was collected from animals and serum was separated via centrifugation. ALT and AST were measured using an ACE Alera Blood Chemistry Analyzer (Alfa Wassermann). All calibrations and bi-level controls were performed according to instrument-specific SOPs.

Lifespan analysis and statistics

Mice were monitored for the development of ascites, impairment of gait and breathing indicative of endstage liver tumors. Survival curves were constructed by the Kaplan-Meier method using GraphPad Prism software. Paired data were analyzed using a 2-tailed paired Student's t test. A P value of less than 0.05 was considered significant.

Results

A tissue-mimicking media to visualize 3-dimensional coagulation temperature distribution during RFA

To optimize the use of RF energy in liver ablation procedures, we used a human-use EPT-1000 XP™ cardiac radiofrequency generator with one probe and 2 ground conductors which are modified to be utilized in mice (**Fig. 1A**) in liver-tissue-mimicking media to measure temperature distribution during RFA with different parameters. The temperature map at the end of a 60 sec RFA application at 65 °C target temperature shows heat immediately surrounding the probes with cooling as distance is increased from the probe (**Fig 1B**). We performed this test at varying target temperatures to verify similar results were obtained (**Fig. 1C**). Assuming that cancer cells are killed above 50°C,[23] we can estimate the diameter of the generated ablation zone to be 5 mm at 65°C, 6 mm at 75°C, and 8 mm at 85°C. Due to blood perfusion mediated cooling, we can expect the ablation zones to be slightly smaller *in vivo*.

Successful focused liver destruction in normal mice with RFA

To test the effect of liver ablation with the modified RFA equipment and defined parameters generated by tissue-mimicking media, RFA with distinct temperatures for 60 s are

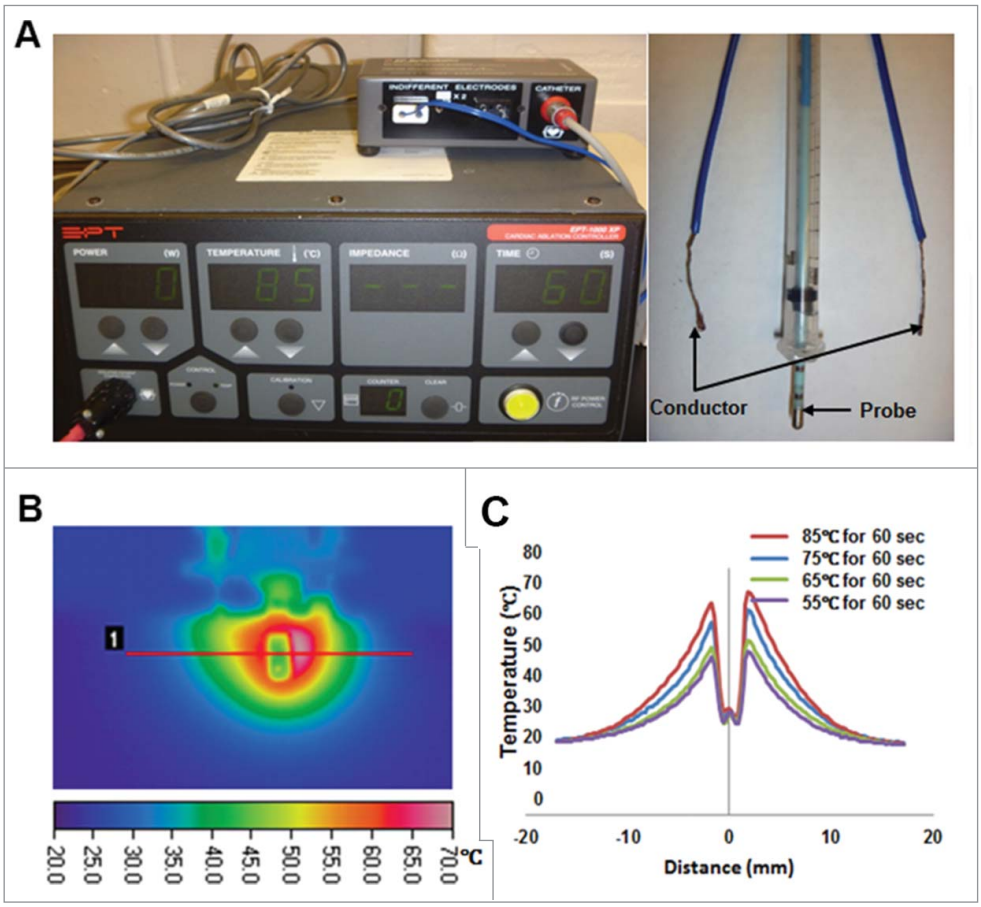

Figure 1. A tissue-mimicking media for optimizing RFA conditions. (A) A EPT-1000 XP™ cardiac RFA generator (left panel) together with a cardiac ablation electrode (4 mm length, 2.33 mm diameter; right panel) were used in this study. Two additional conductors served as ground electrodes (right panel). **(B)** Tissue-mimicking media was used to develop a temperature map after RF heating at a 65°C target temperature for 60 s (left panel). Radial temperature profile after 60 s heating varied with target temperature, with higher temperatures resulting in larger ablation zones (right panel).

Figure 2. Liver ablation of normal mice with RFA. 10 week-old of C57BL/6 mice were given inhalational isoflurane to induce adequate anesthesia, then the abdomen was opened to expose the liver. Two grounding conductors were placed on either side of the opened abdomen. The RFA probe was placed on the liver surface to perform RFA with defined conditions: A power output of maximal 10 W for 60 s was utilized. The temperature of the probe tip was set at 85°C. **(A)** Representative macroscopic pictures of mice which underwent sham and RFA treatment with recovery over time. Mice in the upper panel received laparotomy without RFA treatment were used for sham control. Mice in the lower panel represent animals receiving RFA. **(B)** Accumulated results showed the damaged liver area post RFA. n=3, *p<0.05, error bars represent mean ±SDs.

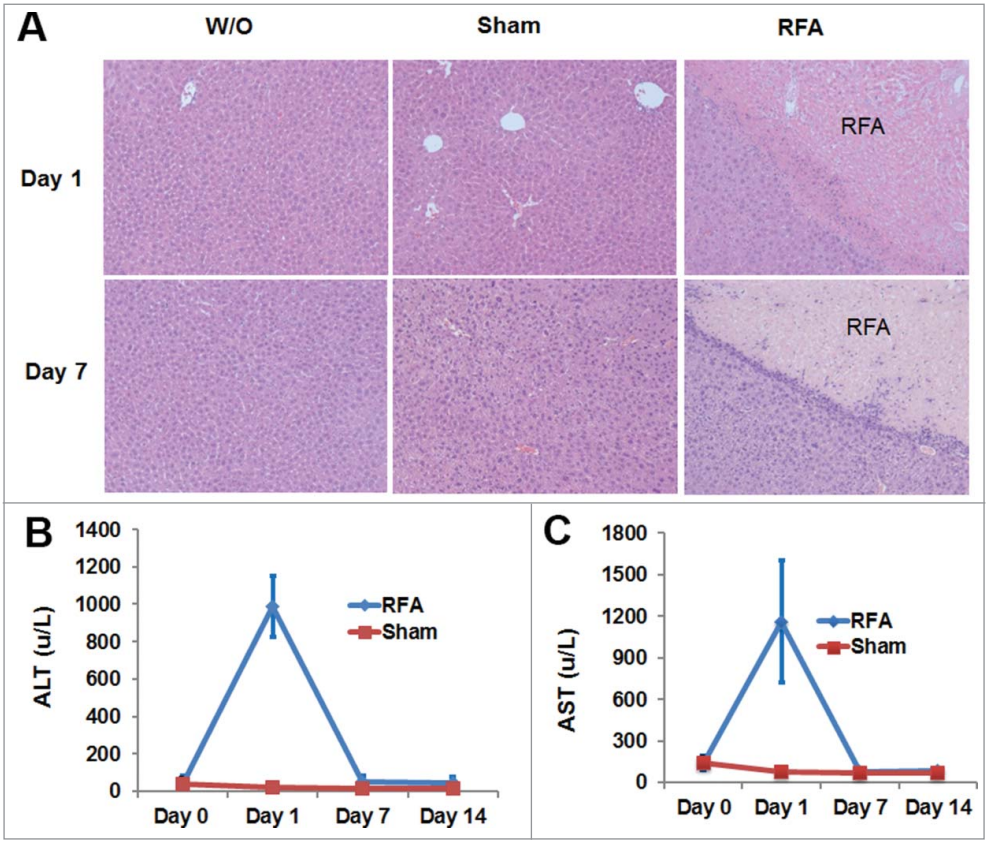

Figure 3. H& E staining of liver tissue and the levels of ALT and AST in the blood of RFA-treated mice. 10 week-old of C57BL/6 mice received RFA treatment as described. Liver tissue was harvested from each mouse to make slides for H & E staining. Serum was collected for ALT and AST measurements. **(A)** Representative H & E staining showed RFA-generated liver damage. **(B)** The level of ALT in the serum from mice with or without RFA treatment. **(C)** The level of AST in the serum from mice with or without RFA treatment. n=3, *p<0.05, error bars represent mean ±SDs.

performed in the liver of normal C57BL/6 mice. As predicted, RFA application at 85°C for 60 s in the liver resulted in an area of tissue destruction slightly smaller than the observed zone of ablation that was achieved in the tissue mimicking media (**Fig. 2A**, lower panel). The zone of liver ablation was assessed by measuring the diameter of the thermally damaged hepatic parenchyma with calipers. The accumulated results from 3 animals at each timepoint were shown in **Figure 2B**. The results suggest that RFA performed at 85°C for 60 s results in uniform and predictable liver damage in an area of approximately 50 mm^2 and at a depth of about 3 mm.

Typical features of the ablated liver and elevated level of ALT and AST in blood of normal mice receiving RFA treatment

To further define the typical features of the ablated area, conventional H&E staining is used for histologic assessment. As shown in **Figure 3A**, demarcation between viable and nonviable tissue is evident in the livers from RFA-treated mice.

ALT and AST are both "leakage" enzymes and are released with hepatocyte damage (either sublethal or overt necrosis). Serum levels depend on the number of cells damaged or the severity of injury. The extent of murine hepatic damage from RFA is evident histologically (**Fig. 3A**) and correlates with elevated levels of ALT and AST. As shown in **Figure 3B-C**, the peak value of ALT and AST in the serum of the RFA-treated mice was detected one day after RFA. This value was significantly higher than that in mice prior to RFA treatment (baseline). Seven days later, levels of ALT and AST were observed to return baseline. In contrast, no significant difference in the level of ALT and AST was detected over time in mice with sham treatment.

Tumor damage by RFA in small and large tumor-bearing mice

Recently, we established a successful MRI protocol to monitor tumor progression and size in wild type mice which received ISPL inoculation of oncogenic hepatocytes from MTD2 mice.[14] Tumor-bearing mice with both small (<120 mm^3) and large tumors (>120 mm^3) were treated with the optimized RFA conditions that were established in wild-type non-tumor bearing mice (**Fig. 4A**). The tumor destruction was assessed through measurement of the damaged areas (**Fig. 4B**). The results suggest that RFA with 85°C for 60 s resulted in successful complete ablation of small tumors; however, the size of the large tumors exceeded the volume of tissue destruction obtained by RFA at 85°C for 60s. Importantly, no bleeding was generated in either small tumors or large tumors with RFA treatment. In addition, MRI was successfully used to monitor tumor ablation on Day 14 after RFA treatment (**Fig. 4C**).

Typical features of the ablated tumors and elevated level of ALT and AST in blood of tumor-bearing mice receiving RFA treatment

To further define the typical features of tumors prior to and post RFA ablation, histologic assessment with conventional H & E staining is performed. H & E staining showed the prominent demarcation between tumor tissue and normal liver tissue. RFA treatment resulted in necrosis of tumor tissue with evident demarcation between viable tumor tissue and RFA-induced non-viable tumor tissue in histologic sections (**Fig. 5**).

The basal level of ALT and AST in the blood of large tumor-bearing mice is 300 u/L, which is markedly higher than that in normal and small tumor-bearing mice (<100 u/L) (**Fig. 5B-C**). RFA treatment induced further elevated levels of ALT and AST in the serum of small and large tumor-bearing mice in comparison to large tumor-bearing mice without RFA treatment. As shown in **Figure 5B-C**, the peak value of ALT and AST in the serum was detected one day after RFA treatment in mice with small and large tumors. Seven days later, levels of ALT and AST returned to baseline.

Therapeutic efficacy of RFA on tumor-bearing mice

We investigated the therapeutic efficacy of RFA in mice bearing small and large tumors. Tumor size in tumor-bearing mice was determined by MRI. Cohorts of mice bearing small tumors of equivalent size were randomly divided into 2 groups which received RFA treatment or sham treatment, and mice with large tumors of similar size were grouped and treated in a similar fashion. Survival analysis revealed 100% mortality in large tumor-bearing mice within 4 months post sham treatment (**Fig. 6**). A parallel cohort of large tumor-bearing mice which received RFA treatment didn't result in significantly increased survival ($p<0.05$). All mice in this cohort were euthanized within 5 months post-RFA treatment, as the tumor burden exceeded pre-set limits. In contrast, a 60% survival rate was achieved in small tumor-bearing mice at 10 months post-RFA treatment, at which point the study was terminated. Endpoints were reached within 6 months in small-tumor bearing animals receiving sham treatment.

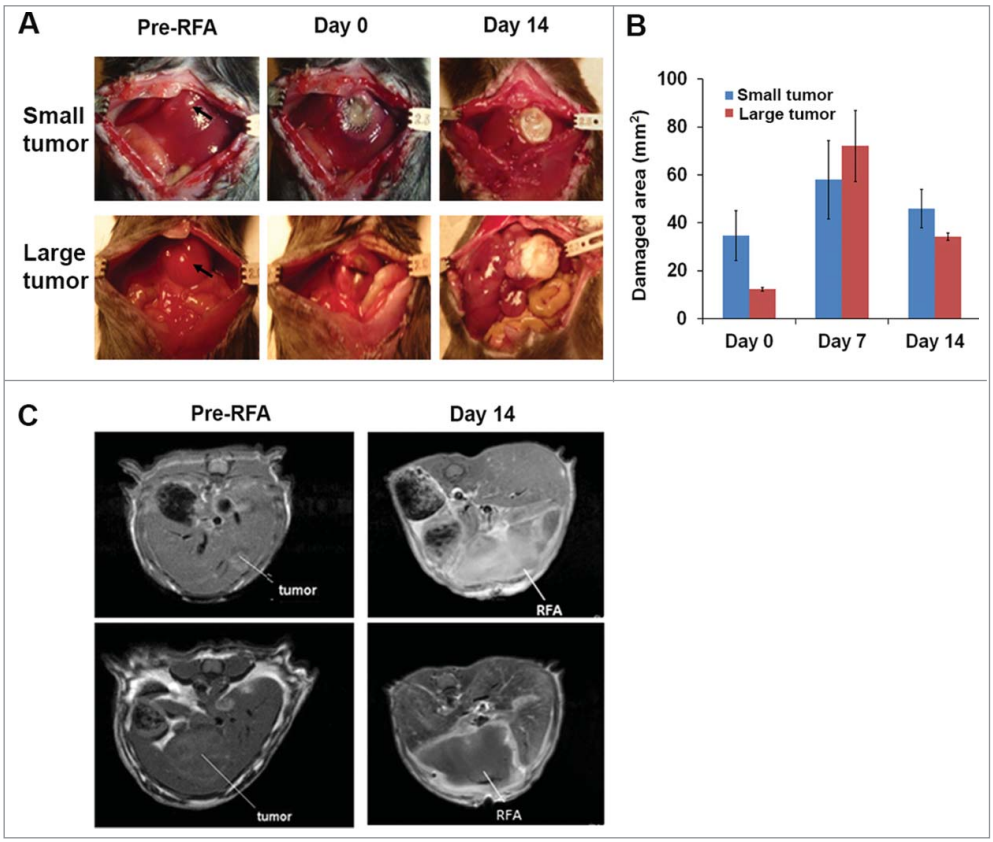

Figure 4. RFA treatment for destroying small and large tumors. Orthotopic murine HCCs were established, and the tumor size was measured with MRI. Mice with small and large tumors were selected to perform RFA with parameters that were previously defined in normal mice. A power output of 10 W for 60 s was utilized in tumor ablation. The temperature of the probe tip was set at 85°C. **(A)** Representative macroscopic pictures showed tumor ablation after RFA treatment. **(B)** Accumulated results demonstrate the damaged liver area post-RFA application. n=3, *$p<0.05$, error bars represent mean ±SDs. **(C)** Representative MRI scans to monitor tumor and RFA-generated tumor damage.

Discussion

In this study, we have established a successful RFA platform for the treatment of HCC in a relevant, orthotopic murine model. Successful RFA is demonstrated to significantly extend overall survival of small tumor-

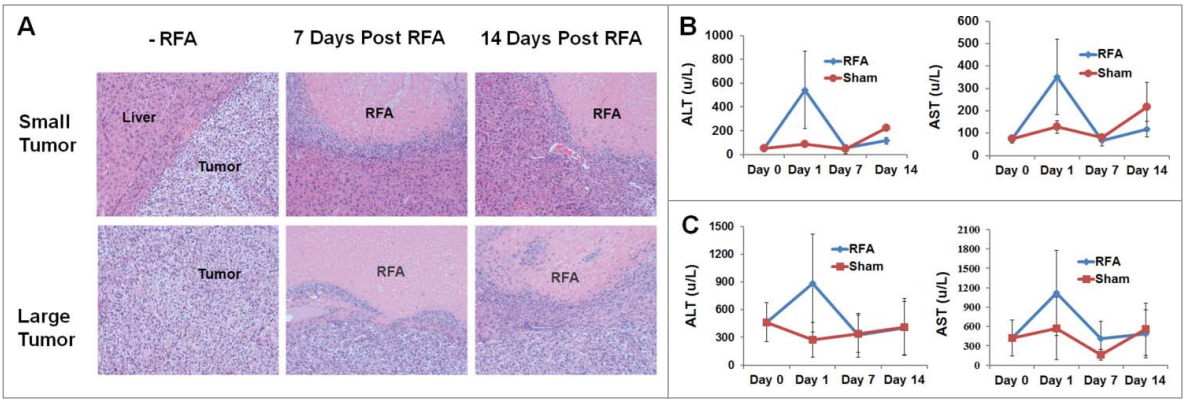

Figure 5. Characteristics of tumor damage induced by RFA treatment. Mice bearing small and large tumors of equivalent size received RFA treatment or sham treatment. Tumor tissue was harvested from each mouse from the respective treatment groups at distinct set time periods and slides were prepared for H & E staining. Simultaneously, serum was collected for ALT and AST measurements. **(A)** Representative H & E staining showed RFA-generated tumor damage in mice bearing small and large tumors. **(B)** The level of ALT and AST in the serum from small tumor-bearing mice receiving RFA and control sham treatment. **(C)** The level of ALT and AST in the serum from large tumor-bearing mice receiving RFA and control sham treatment. n=3, *p<0.05, error bars represent mean ±SDs.

bearing mice, but only marginally increase overall survival of large tumor-bearing mice (**Fig. 6**). This in vivo system provides a unique opportunity to study RFA in murine models, allowing for development of more efficient therapeutic approaches and overcome the limitations of current RFA treatments in patients with HCC.

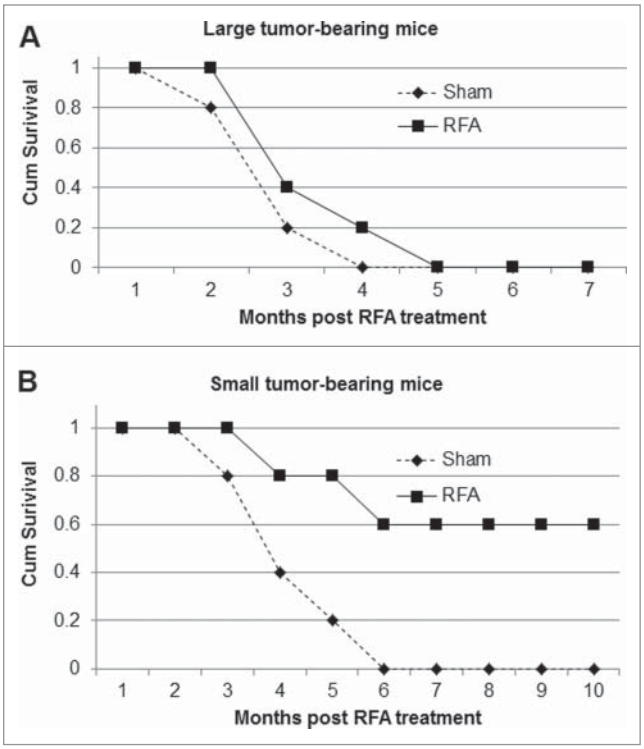

Figure 6. The monotherapeutic efficacy of RFA on small and large tumor-bearing mice. Mice bearing small and large tumors of equivalent size were divided into 2 groups which received RFA treatment or control sham treatment. The survival of mice bearing small tumors **(A)** and large tumors **(B)** post-RFA treatment was observed over time.

An important contribution of the present study is the successful application of RFA in mice bearing either small or large tumors.[24] This treatment mimics human clinical scenarios of both complete and incomplete ablation, as ablation was more effective in small tumors when compared to the effects of ablation on larger tumors (**Fig. 4**).[24] The damage produced is dependent on both the temperature achieved within the tissue and the length of exposure to the heating process (**Fig. 1**). Despite the lack of a dedicated RF generator designed for murine applications, an EPT-1000 XP^{TM} cardiac radiofrequency generator equipped with a 4 mm cardiac ablation probe (7F/2.33 mm diameter) was modified to perform successful liver or tumor ablations in mice after 2 ground conductors were separated and placed either side of open abdomen. We demonstrate that targeted temperatures from 55°C to 85°C with a 60 s exposure time resulted in successful tumor damage with zones of ablation that increased corresponding to the increase in the temperature applied. Only a one time RFA performed at 85°C for 60 s resulted in complete small tumor ablation. In contrast, a one time RFA treatment only induced partial damage to large tumors and was ineffective in preventing tumor progression.

The utilization of a clinically relevant murine model of HCC and successful RFA treatment provide a unique opportunity to develop new and effective RFA-integrated immunotherapeutic approaches.[25] RFA monotherapy is only clinically applicable to patients with small tumors and limited disease; furthermore, local ablation strategies may result in local tumor recurrence and do not address distant recurrences. Recently, combinational strategies incorporating RFA with immunotherapies (vaccination[26] or the administration of IL-2[27]) have demonstrated improvements in the treatment of HCC. In the present study, ISPL inoculation of histologically normal oncogenic hepatocytes into

immunocompetent mice is used to induce spontaneous tumor growth in wild type mice with intact immune systems. We have demonstrated that immune tolerance occurs in large tumor-bearing mice. Furthermore, we have observed that tolerance is accompanied with a pronounced and enhanced expression of cytotoxic T-lymphocyte-associated antigen-4 (CTLA-4) and programmed death-1 (PD-1) in tumor-infiltrating CD4 and CD8 T cells (unpublished data). Recent advances in the treatment of metastatic melanoma have been achieved by blocking immune checkpoints. Ipilimumab, an anti-CTLA-4 monoclonal antibody,[28] and nivolumab, an anti-PD-1 monoclonal antibody,[29,30] are approved by the FDA on the basis of improvement in overall survival among patients with advanced melanoma. In addition, a recent phase I/II nivolumab trial demonstrated anti-tumor activity in patients with HCC. We are hopeful that the combination of RFA and blockade of immune checkpoints may overcome the limitations of either monotherapy and generate a more powerful therapeutic strategy in HCC.[31] The successful RFA platform established in the present study provides our team with a unique opportunity to test this hypothesis.

We demonstrated that RFA induces acute liver or tumor damage and results in a quick elevation of ALT and AST in the blood of the treated mice. The elevated ALT and AST speedily return to baseline levels indicating that there is no further tissue damage after the initial insult. Thus, monitoring levels of ALT and AST may provide a useful guide to optimize the timing of subsequent treatment post-RFA.

We also demonstrated that tissue-mimicking media is clinically useful to define parameters for RFA treatment. In this study, we utilized a tissue-mimicking media to evaluate the ablation zone at varying temperatures, and provide guidelines for treatment based on optimal treatment parameters (temperature, time). The optimized RFA parameters resulted in zones of ablation which were slightly smaller when applied to tumors in our orthotopic murine tumor model.

In summary, the creation of an experimental RFA platform with our orthotopic murine model and a readily available human RF generator provides an opportunity to advance the study of RFA in HCC. Utilization of an orthotopic murine model with immunocompotent wild-type mice and specific tumor antigens 445 uniquely positions us to develop more powerful RFA-integrated approaches in combination with other treatments, including immunotherapies.

Disclosure of Potential Conflicts of Interest

No potential conflicts of interest were disclosed.

Acknowledgments

The authors thank Xingju Nie and Margaret Romano for expert technical assistance.

Funding

Grant Support: 1 R01 CA164335-01A1 (K. F. Staveley-O'Carroll, PI) from the National Cancer Institute/National Institutes of Health; In part by an ACS-IRG pilot research funding from an American Cancer Society Institutional Research Grant awarded to the Hollings Cancer Center, Medical University of South Carolina (Guangfu Li, PtdIns).

References

1. Centers for Disease Control and Prevention (CDC). Hepatocellular carcinoma - United States, 2001-2006. MMWR Morb Mortal Wkly Rep 2010; 59:517-20; PMID:20448528
2. Wang L, Liu M, Zhu H, Rong W, Wu F, An S, Liu F, Feng L, Wu J, Xu N. Identification of recurrence-related serum microRNAs in hepatocellular carcinoma following hepatectomy. Cancer Biol Ther 2015; 16 (10):1445-52
3. Njei B, Rotman Y, Ditah I, Lim JK. Emerging trends in hepatocellular carcinoma incidence and mortality. Hepatology 2015; 61:191-9; PMID:25142309; http://dx.doi.org/10.1002/hep.27388
4. Perz JF, Armstrong GL, Farrington LA, Hutin YJ, Bell BP. The contributions of hepatitis B virus and hepatitis C virus infections to cirrhosis and primary liver cancer worldwide. J Hepatol 2006; 45:529-38; PMID:16879891; http://dx.doi.org/10.1016/j.jhep.2006.05.013
5. Yang JD, Roberts LR. Hepatocellular carcinoma: A global view. Nat Rev Gastroenterol Hepatol 2010; 7:448-58; PMID:20628345; http://dx.doi.org/10.1038/nrgastro.2010.100
6. Zak Y, Rhoads KF, Visser BC. Predictors of surgical intervention for hepatocellular carcinoma: race, socioeconomic status, and hospital type. Arch Surg 2011; 146:778-84; PMID:21422327; http://dx.doi.org/10.1001/archsurg.2011.37
7. Chen X, Chen Y, Li Q, Ma D, Shen B, Peng C. Radiofrequency ablation versus surgical resection for intrahepatic hepatocellular carcinoma recurrence: a meta-analysis. J Surg Res 2015; 195:166-74; PMID:25724768; http://dx.doi.org/10.1016/j.jss.2015.01.042
8. Chok K. Management of recurrent hepatocellular carcinoma after liver transplant. World J Hepatol 2015; 7:1142-8; PMID:26052403; http://dx.doi.org/10.4254/wjh.v7.i8.1142
9. Llovet JM, Di Bisceglie AM, Bruix J, Kramer BS, Lencioni R, Zhu AX, Sherman M, Schwartz M, Lotze M, Talwalkar J, et al. Design and endpoints of clinical trials in hepatocellular carcinoma. J Natl Cancer Inst 2008; 100:698-711; PMID:18477802; http://dx.doi.org/10.1093/jnci/djn134
10. Haemmerich D. Biophysics of radiofrequency ablation. Crit Rev Biomed Eng 2010; 38:53-63; PMID:21175403; http://dx.doi.org/10.1615/CritRevBiomedEng.v38.i1.50
11. Zhong JH, Ma L, Li LQ. Postoperative therapy options for hepatocellular carcinoma. Scand J Gastroenterol 2014; 49:649-61; PMID:24716523; http://dx.doi.org/10.3109/00365521.2014.905626
12. Bakiri L, Wagner EF. Mouse models for liver cancer. Mol Oncol 2013; 7:206-23; PMID:23428636; http://dx.doi.org/10.1016/j.molonc.2013.01.005
13. Bimonte S, Barbieri A, Palaia R, Leongito M, Albino V, Piccirillo M, Arra C, Izzo F. An overview of locoregional treatments in patients and mouse models for hepatocellular carcinoma. Infect Agent Cancer 2015; 10:9; PMID:25755676; http://dx.doi.org/10.1186/s13027-015-0004-2
14. Avella DM, Li G, Schell TD, Liu D, Zhang SS, Lou X, Berg A, Kimchi ET, Tagaram HR, Yang Q, et al. Regression of established hepatocellular carcinoma is induced by chemoimmunotherapy in an orthotopic murine model. Hepatology 2012; 55:141-52; PMID:21898502; http://dx.doi.org/10.1002/hep.24652
15. Michelotti GA, Xie G, Swiderska M, Choi SS, Karaca G, Krüger L, Premont R, Yang L, Syn WK, Metzger D, et al. Smoothened is a master regulator of adult liver repair. J Clin Invest 2013; 123:2380-94; PMID:23563311
16. Curley SA. Radiofrequency ablation of malignant liver tumors. Oncologist 2001; 6:14-23; PMID:11161225; http://dx.doi.org/10.1634/theoncologist.6-1-14
17. Bertrand J, Caillol F, Borentain P, Raoul JL, Heyries L, Bories E, Pesenti C, Ratone JP, Bernard JP, Gerolami R, et al. Percutaneous hepatic radiofrequency for hepatocellular carcinoma: results and outcome of 46 patients. Hepat Med 2015; 7:21-7; PMID:26056497; http://dx.doi.org/10.2147/HMER.S67940
18. Fukushima T, Ikeda K, Kawamura Y, Sorin Y, Hosaka T, Kobayashi M, Saitoh S, Sezaki H, Akuta N, Suzuki F, et al. Randomized Controlled Trial Comparing the Efficacy of Impedance Control and Temperature Control of Radiofrequency Interstitial Thermal Ablation for Treating Small Hepatocellular Carcinoma. Oncology 2015; 89:47-52; PMID:25790846; http://dx.doi.org/10.1159/000375166
19. Tevethia SS, Greenfield RS, Flyer DC, Tevethia MJ. SV40 transplantation antigen: relationship to SV40-specific proteins. Cold Spring Harb Symp Quant Biol 1980; 44 Pt 1:235-42; PMID:6253137; http://dx.doi.org/10.1101/SQB.1980.044.01.027
20. Schirmacher P, Held WA, Yang D, Biempica L, Rogler CE. Selective amplification of periportal transitional cells precedes formation of hepatocellular carcinoma in SV40 large tag transgenic mice. Am J Pathol 1991; 139:231-41; PMID:1649555
21. Haemmerich D, Schutt DJ. RF ablation at low frequencies for targeted tumor heating: in vitro and computational modeling results. IEEE Trans Biomed Eng 2011; 58:404-10; PMID:20934940; http://dx.doi.org/10.1109/TBME.2010.2085081

22. Feld G, Wharton M, Plumb V, Daoud E, Friehling T, Epstein L. Radiofrequency catheter ablation of type 1 atrial flutter using large-tip 8- or 10-mm electrode catheters and a high-output radiofrequency energy generator: results of a multicenter safety and efficacy study. J Am Coll Cardiol 2004; 43:1466-72; PMID:15093885; http://dx.doi.org/10.1016/j.jacc.2003.11.036
23. Reddy G, Dreher MR, Rossmann C, Wood BJ, Haemmerich D. Cytotoxicity of hepatocellular carcinoma cells to hyperthermic and ablative temperature exposures: in vitro studies and mathematical modelling. Int J Hyperthermia 2013; 29:318-23; PMID:23738699; http://dx.doi.org/10.3109/02656736.2013.792125
24. Lee DH, Lee JM, Lee JY, Kim SH, Yoon JH, Kim YJ, Han JK, Choi BI. Radiofrequency ablation of hepatocellular carcinoma as first-line treatment: long-term results and prognostic factors in 162 patients with cirrhosis. Radiology 2014; 270:900-9; PMID:24475823; http://dx.doi.org/10.1148/radiol.13130940
25. Burke CT, Cullen JM, State A, Gadi S, Wilber K, Rosenthal M, Bulysheva A, Pease A, Mauro MA, Fuchs H. Development of an animal model for radiofrequency ablation of primary, virally induced hepatocellular carcinoma in the woodchuck. J Vasc Interv Radiol 2011; 22:1613-8 e1; PMID:21959057; http://dx.doi.org/10.1016/j.jvir.2011.08.020
26. Nobuoka D, Yoshikawa T, Sawada Y, Fujiwara T, Nakatsura T. Peptide vaccines for hepatocellular carcinoma. Hum Vaccin Immunother 2013; 9:210-2; PMID:23442593; http://dx.doi.org/10.4161/hv.22473
27. Lee JH, Lee JH, Lim YS, Yeon JE, Song TJ, Yu SJ, Gwak GY, Kim KM, Kim YJ, Lee JW, et al. Adjuvant immunotherapy with autologous cytokine-induced killer cells for hepatocellular carcinoma. Gastroenterology 2015; 148:1383-91 e6; PMID:25747273; http://dx.doi.org/10.1053/j.gastro.2015.02.055
28. Camacho LH. CTLA-4 blockade with ipilimumab: biology, safety, efficacy, and future considerations. Cancer Med 2015; 4:661-72; PMID:25619164; http://dx.doi.org/10.1002/cam4.371
29. Postow MA, Chesney J, Pavlick AC, Robert C, Grossmann K, McDermott D, Linette GP, Meyer N, Giguere JK, Agarwala SS, et al. Nivolumab and ipilimumab versus ipilimumab in untreated melanoma. N Engl J Med 2015; 372:2006-17; PMID:25891304; http://dx.doi.org/10.1056/NEJMoa1414428
30. Wilkinson E. Nivolumab success in untreated metastatic melanoma. Lancet Oncol 2015; 16:e9; PMID:25638562; http://dx.doi.org/10.1016/S1470-2045(14)71129-5
31. Chen Y, Ramjiawan RR, Reiberger T, Ng MR, Hato T, Huang Y, Ochiai H, Kitahara S, Unan EC, Reddy TP, et al. CXCR4 inhibition in tumor microenvironment facilitates anti-programmed death receptor-1 immunotherapy in sorafenib-treated hepatocellular carcinoma in mice. Hepatology 2015; 61:1591-602; PMID:25529917; http://dx.doi.org/10.1002/hep.27665